Journal of Applied Fluid Mechanics, Vol. 16, No. 12, pp. 2316-2328, 2023.
Available online at www.jafmonline.net, ISSN 1735-3572, EISSN 1735-3645.
https://doi.org/10.47176/jafm.16.12.2092

Computational Study on the Effect of Vane Design in Enhancing the Mixing of Subsonic Jet and Sonic Jet

S. Thanigaiarasu[1†], G. Balamani[1], K. Mirnal[2] and K. Revathy[3]

[1] *Department of Aerospace Engineering, MIT Campus, Anna University, Chennai 600044, India*
[2] *Department of Aerospace Engineering, IIT Kharagpur 721302, India*
[3] *Department of Aerospace Engineering, IIT Kanpur 208016, India*

†*Corresponding Author Email: sthanigaiarasu@mitindia.edu*

ABSTRACT

The purpose of this study is to numerically analyze the effect of vortex generators that are shaped like vanes in enhancing the mixing of subsonic and sonic jet and to determine the best design which yields maximum reduction in jet potential core length and minimum thrust loss at the nozzle exit. Four different nozzle designs namely, models A, B, C and D are designed and compared with a base nozzle which is a plain circular nozzle without any vanes. The simulation is performed in ANSYS Fluent using the S-A turbulence model. The centerline pressure decay and radial pressure decay from models A to D are compared with that of the base nozzle to determine the ability of the vane to enhance the jet mixing characteristics. To evaluate the thrust loss, the total pressure at the exit plane of models A to D is measured and compared with that of the base nozzle. When comparing all the designs, it is observed that Model B produces the highest reduction in potential core length which is 66.4% at Mach no. 1 and Model D produces minimum total pressure loss which is 0.47% at Mach no. 0.4. In contrast to the conventional method, this design introduces a novel approach by placing the vanes parallel to the flow instead of the usual perpendicular arrangement. This unique configuration allows the vanes to redirect the flow rather than hinder it, resulting in a total pressure loss of less than 3%.

Article History

Received June 11, 2023
Revised July 17, 2023
Accepted July 25, 2023
Available online October 8, 2023

Keywords:

Jet mixing
Jet control
Turbulent flows
Vanes
Vortices
Vortex generators
Mixing enhancement
Thrust loss

1. INTRODUCTION

In the field of jet control, passive control methods are widely used because it requires no external power. The passive control techniques mostly make use of geometrical changes in the location of flow separation. Numerous studies have focused on the placement of vortex generators at the exit of the nozzle as a means of passive jet control mechanism (Rathakrishnan, 2019).

The earliest to study the effect of vortex generators such as vanes which are placed parallel to the flow direction was Powell (1954). He analyzed the usage of cambered radial vanes at the nozzle exit, which generated tip vortices and caused the flow to rotate to about 5° thereby enhancing the jet mixing capability and thus reducing the subsonic jet noise. Hence, it is clear that vanes can enhance the jet mixing characteristics.

Another vortex generator that is aligned parallel to the flow is called notches which are v-shaped cut-outs positioned near the nozzle exit in the axial direction. Pannu and Johannessen (1976) found that in the notched plane there was a very marked fanning out of the outer part of the jet. Grooves are geometries that are also similar to notches. In the investigation of nozzles with internal grooves by Elangovan and Rathakrishnan (2004), it was determined that the jet spread along the grooved plane was larger than that along the ungrooved plane and the jet from the grooved nozzle has a shorter core length with faster decay both in the near and far-field compared to that of the plain nozzle (Vishnu & Rathakrishnan, 2003). It was found by Ishii et al., (2011) that the size and the number of vortex generators also play an important role in enhancing the jet mixing properties. Mali et al. (2023) showed that the grooves induce significant distortions in the jet structure, leading to substantial mass entrainment and lateral spread.

Another type of vortex generator which are placed perpendicular to the flow direction is tabs. The mixing enhancing capability of tabs (Bradbury & Khadem, 1975) has been extensively studied and the effect of various

Nomenclature			
D	nozzle exit diameter	k	Turbulence Kinetic energy
M	Mach number	U	Mean Velocity
P_{0i}	Nozzle inlet total pressure	σ	Turbulent Prandtl number
P_{0e}	Nozzle exit total pressure	ν_T	Kinematic eddy Viscosity
X	distance along jet axial direction	u_i	mean velocities in xi directions
Y	distance along jet radial (lateral) direction	$u'i$	velocity fluctuations in the xi direction
Z	distance along jet radial (vertical) direction	S	Strain rate scalar

design modifications of tabs (Patil and Rathakrishnan, 2019; Thanigaiarasu et al. (2008); Chand et al. (2011); Dhakshnamoorthy et al., (2014); Maruthupandiyan and Rathakrishnan, (2018); Akram and Rathakrishnan, (2017) and Ezhilmaran et al. (2019); Thangaraj et al. (2022) has also been previously studied and it has been concluded that tabs are effective in enhancing the jet mixing characteristics. One such study by Thanigaiarasu et al. (2008) considered the changes in the tab geometry and orientation. It was proved that the pressure gradient produced by the tab concave surface facing the flow was the reason to enhance jet mixing characteristics compared to the other two configurations considered in that study. Moorthi et al. (2023) compared the effect of triangular tabs and rectangular tabs at 90° and 180° intervals and concluded that the core length reductions achieved by the triangular tabs were generally higher than those of the rectangular tabs at both intervals. Richards et al. (2023) investigated the effect of tabs with asymmetric projections which leads to the generation of counter-rotating vortices, causing shear distortions and instability at the nozzle exit, resulting in significant reductions in core length and asymmetrical total pressure decay characteristics.

The existing literature extensively covers the use of perpendicular vortex generators for jet mixing enhancement, but these generators often lead to significant thrust loss due to flow obstruction (Rathakrishnan, 2019). However, Gandhinathan and Subramanian (2022) demonstrated that vanes can effectively enhance jet mixing while minimizing thrust loss. In this study, we explore the potential of vanes with different dimensions, differing from those used in the aforementioned work. This study investigates the effects of different vane configurations, involving variations in both the number of vanes and their lengths, on jet characteristics. By placing the vanes axially along the flow direction, they redirect the flow at an angle rather than obstructing it, resulting in minimal thrust loss. Notably, Powell (1954) suggests that these vanes generate tip vortices with high vorticity and downwash, leading to a broader jet spread—an essential characteristic for jet mixing enhancement. This study analyses the effect of the vane's length and the number of vane to assess their impact on jet characteristics.

Therefore, the primary research question of this study is: "How do different vane configurations, varying in length and number, affect jet characteristics and enhance mixing in subsonic and sonic jets?" Furthermore, we hypothesize that the inclusion of vanes in the nozzle design will lead to a reduction in the potential core length of the jet and minimize thrust loss at the nozzle exit, providing an efficient and effective passive control method for jet mixing enhancement. Consequently, a detailed numerical analysis has been carried out with vanes of various dimensions placed along the flow direction inside the nozzle at the exit to study the mixing enhancement and the jet evolution.

2. METHODOLOGY

2.1 Flow Around the Vane

To understand how the vanes, influence the flow and how vortices are formed due to the presence of the vanes, a simulation was performed to visualize the flow around a vane with a 0 mm radius of curvature and another vane with a 20 mm radius of curvature. A 2D domain of length 30L and height 15L was created where L is the length of the vane. The domain for the straight vane is shown in Fig. 1. A similar domain was created for the curved vane also. A grid Independence study was performed and a grid with 2 lakh elements was finalized. S-A turbulence model was used to carry out the analysis and the reason for choosing the S-A model is explained in upcoming sections.

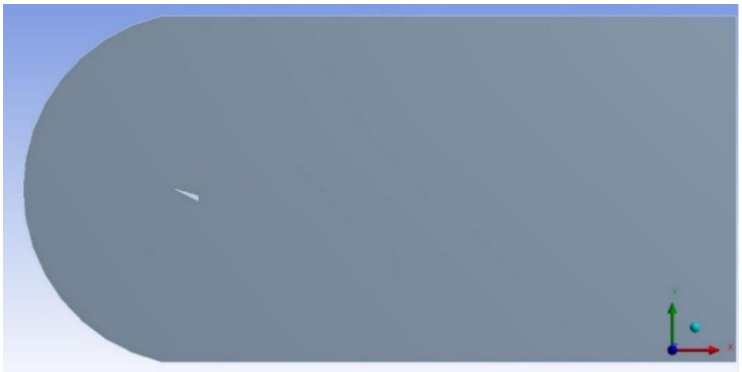

Fig. 1 Computational Domain for Straight Vane

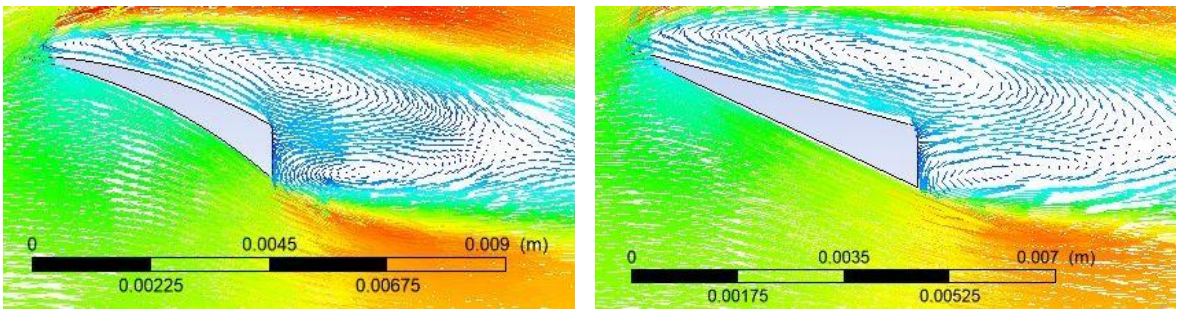

a) b)

Fig. 2 Velocity vector plot of flow around (a) Curved Vane, (b) Straight Vane

Table 1 Attributes of the different Nozzle Configurations

Model	No. of Vanes	Radius of Curvature (mm)	Length of the vanes (mm)	Height and Width (mm)
Base	Nil	Nil	Nil	2 x 2
A	12	20	7.5	2 x 2
B	6	20	7.5	2 x 2
C	12	20	5	2 x 2
D	6	20	5	2 x 2

The vector plot around the vane was captured and is shown in Fig 2a and 2b. From Fig 2, it can be seen that the flow separates on the upper surface of the vanes near the leading edge itself which rolls up to create vortices. The flow in the bottom surface remains attached to a certain distance and then it is separated leading to the formation of vortices near the trailing edge. The interaction of the flow from the upper surface with the flow from the bottom surface near the trailing edge leads to shear action. It has been established that the jet undergoes fine-scale mixing at the corners and high curvature regions and large suction at the low curvature/flat side regions owing to the formation of large-scale vortices, resulting in large entrainment (Rathakrishnan, 2019).

It is well known that, for mixing enhancement, the jet should have the mass entraining large-scale vortices and mass transporting small-scale vortices in proper proportions. Also, mass transporting or mixing-promoting small-scale vortices of mixed size will result in an immense mixing enhancement. (Rathakrishnan, 2019) The vane can shed both small and large-scale vortices, owing to the presence of sharp corners. Thus, the geometry of the vane proves to be a great advantage in promoting the jet mixing characteristics.

Even though both the vanes shed vortices of a similar pattern the size of the vortices shed from the curved vanes was much bigger than that shed from the straight vane which is due to the effect of radius of curvature. This is in accordance with the vortex theory which states that the size of the vortex shed from an edge is proportional to the radius of curvature of the edge (Aravindh & Rathakrishnan, 2017). Hence, the usage of curved vanes in the nozzle for jet mixing enhancement is studied in detail in the upcoming sections

2.2 Design

For this study five different models are considered including a plain circular convergent nozzle (base nozzle) and four nozzles with vanes that are positioned on the inside surface of the nozzle near the exit. The base nozzle has an outlet diameter of 20 mm, and a convergence angle of 7°. Model A to D also have the same dimensions but they are designed with the vanes. The details of the variations considered in the vane designs are presented in Table 1. The isometric view of the various nozzle models considered is shown in Fig 3.

2.3 Fluid Domain and Meshing

In this study, ANSYS FLUENT 16, a powerful computational fluid dynamics (CFD) software, was utilized to investigate the impact of vane configurations on jet mixing enhancement. It offers comprehensive modeling capabilities for incompressible and compressible flows, with a broad range of mathematical models for transport phenomena. The pressure-based solver mode was employed to analyze the flow. ANSYS FLUENT's turbulence models, including the widely used Spalart-Allmaras model, provide accurate results for aerospace applications involving boundary layers and adverse pressure gradients. Its advanced features, such as parallel processing and double precision, ensure efficient and precise simulations. The software's versatility played a vital role in conducting this comprehensive investigation into vane effects on jet characteristics.

The computational domain consists of two distinct cylindrical regions, as illustrated in Fig 4. This approach of employing two domains was chosen strategically to optimize computational resources. The inner domain, responsible for capturing the flow details where vane-induced effects are prominent, has a length of 15D and a diameter of 10D. On the other hand, the outer domain, encompassing the entire flow field, has a length of 30D and a diameter of 20D.

Unstructured meshes are generated for both domains to ensure accurate representation of complex flow phenomena, particularly around the vanes. The inner domain employs an element size of 0.25 mm, thereby

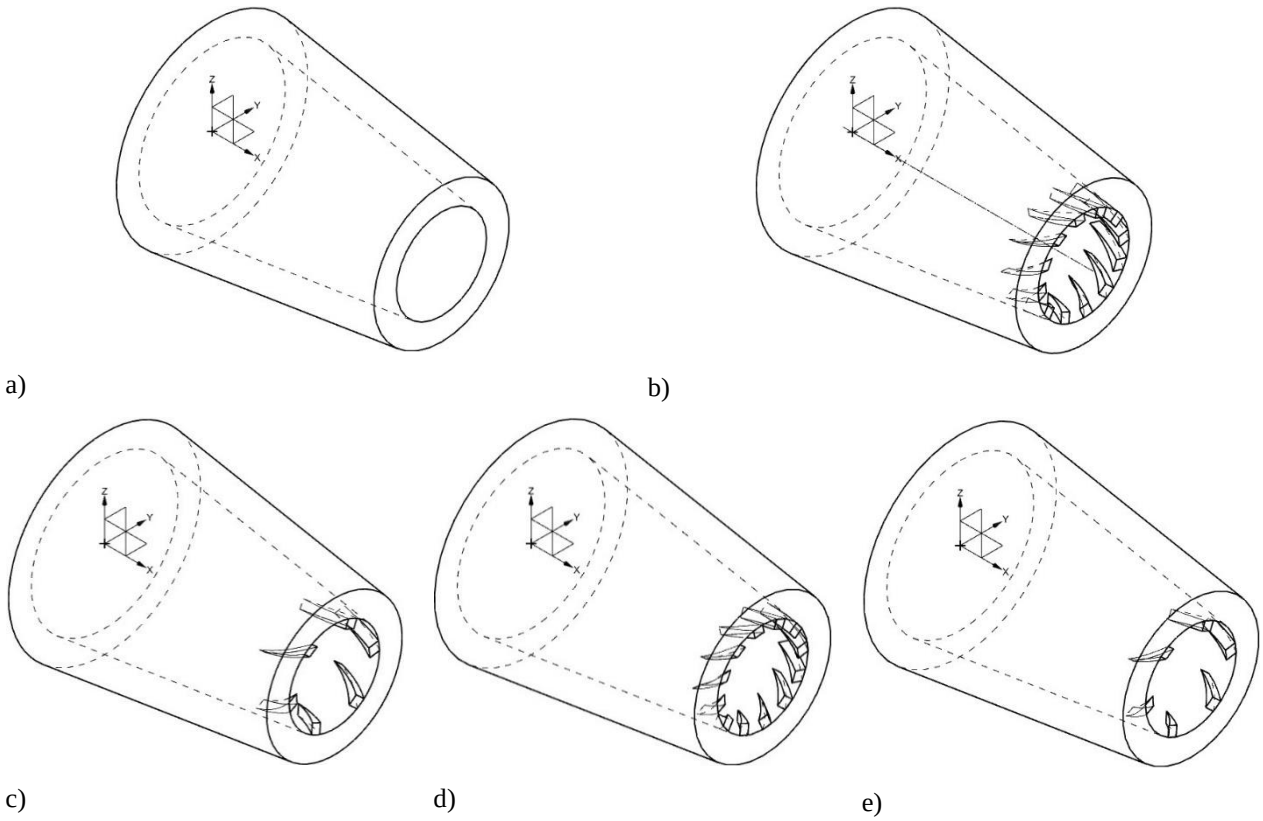

Fig. 3 Isometric View of the Nozzle Designs: a) Base, b) Model A, c) Model B, d) Model C, e) Model D

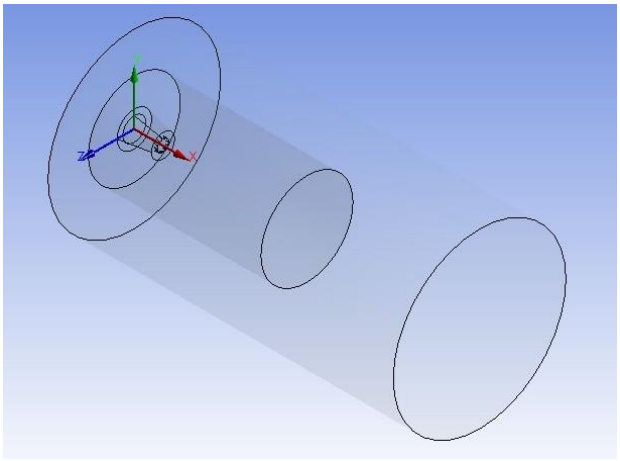

Fig. 4 Computational domain of the nozzle

maintaining a finer mesh to resolve intricate flow features where vane-induced mixing occurs. Simultaneously, the outer domain utilizes a coarser element size of 0.5 mm to achieve computational efficiency and reduce the overall number of mesh elements. This mesh configuration strikes a balance, enabling precise simulation results without excessive computational demands.

In this analysis, the Spalart-Allmaras turbulence model is used, which is a wall function based model and to ensure accurate predictions near the walls and vanes, it is essential to maintain the y+ value between 30 and 200. A y+ value of 30 was chosen, resulting in a first cell thickness of 0.07 mm to adequately capture the boundary layer flow. Inflation was applied near the walls with a first cell thickness of 0.07 mm and a growth rate of 1.2 to capture boundary layer effects. Additionally, edge sizing was used to control the element size around the vanes, ensuring a finer mesh in this region to accurately capture vane-induced mixing.

2.3.1 Grid Independence Study

A grid independence study was performed to evaluate the effect of mesh resolution on the simulation results. three different mesh resolutions were tested which resulted in grid with 30 lakh elements, 50 lakh elements, and 85 lakh elements. The centerline pressure decay was used as the benchmark for comparison of results. The study revealed that the results for the grid with 50 lakh

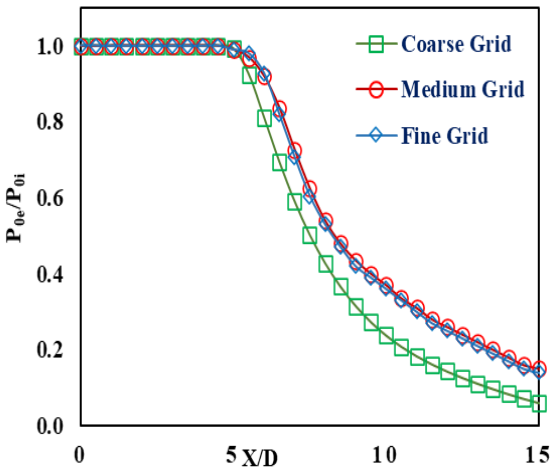

Fig. 5 Grid Independence Study at M = 0.4

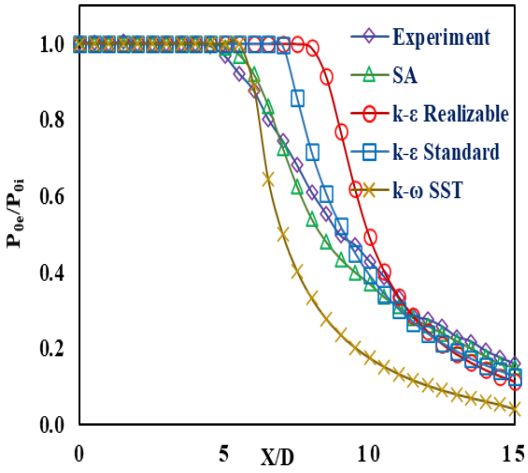

Fig. 6 Validation of the Turbulence Models

elements and the grid with 85 lakh elements were almost identical (Fig. 5). As a result, the 50-lakh element grid was chosen as the optimal mesh resolution for the simulation.

In the conducted grid independence study, vortex generators were included in the cases analyzed. Different grids were employed to account for the varying turbulence models used, and the grid independence study was performed for each configuration. However, in this paper, only one sample grid is presented for clarity. Additionally, the mesh resolution was adapted for different Reynolds number cases, ensuring suitable resolution for each scenario. The meshing process was carefully tailored to suit the specific Reynolds number requirements. While this paper highlights one particular case, the comprehensive study considered various mesh configurations for the turbulence models and Reynolds number variations.

2.4 Choice of Turbulence Model

The analysis is carried out using Spalart-Allmaras (SA) turbulence model (Spalart & Allmaras, 1992). The SA model is a one-equation model that solves a modeled transport equation for the kinematic eddy turbulent viscosity. The SA model has been extensively used by several researchers in the past years (Reddy & Zaman, 2006; Chauvet et al., 2007; Wan & Yu, 2013; Naren et al., 2016) and has been proven to yield accurate results.

From the comparison of simulation results with the experimental data (Fig 6.), it was found that the SA turbulence model produced results that were closest to the experimental data. The SA model accurately predicted the centerline pressure decay in both the potential core region and the far-field, whereas the k-epsilon standard and realizable models over-predicted the potential core region, although they matched the experimental data in the far-field.

The Spalart-Allmaras model is a single-equation turbulence model used to calculate kinematic eddy viscosity. It falls under the class of one-equation models, eliminating the need for determining a length scale associated with local shear layers. Specifically designed for aerospace applications near walls, it has shown robust performance in adverse pressure gradient boundary layer simulations. The model can be adapted to use wall functions for coarse simulations. Moreover, its near-wall gradients are smaller, potentially making it less sensitive to numerical errors in non-layered mesh configurations near walls. The model solves a transport equation for a modified form of turbulent kinematic viscosity.

The defining equations of the SA model is as follows (Wilcox, 1993)

Kinematic Eddy Viscosity

$$v_T = \bar{v} f_{v1} \tag{1}$$

Eddy Viscosity Equation

$$\frac{\partial \bar{v}}{\partial t} + U_j \frac{\partial \bar{v}}{\partial x_j} = c_{b1} \tilde{S} \bar{v} - c_{w1} f_w \left(\frac{\bar{v}}{d}\right)^2 + \frac{1}{\sigma} \frac{\partial}{\partial x_k} \left[(v + \bar{v}) \frac{\partial \bar{v}}{\partial x_k} \right] + \frac{c_{b2}}{\sigma} \frac{\partial \bar{v}}{\partial x_k} \frac{\partial \bar{v}}{\partial x_k} \tag{2}$$

Closure Coefficients

$$c_{b1} = 0.1355, c_{b2} = 0.662, c_{v1} = 7.1, \sigma = 2/3 \tag{3}$$

$$c_{w1} = \frac{c_{b1}}{k^2} + \frac{(1 + c_{b2})}{\sigma}, c_{w2} = 0.3, c_{w3} = 2, k = 0.41 \tag{4}$$

Auxiliary Equations

$$f_{v1} = \frac{X^3}{X^3 + c_{v1}^3}, f_{v1} = 1 - \frac{X}{1 + X f_{v1}}, f_w = g \left[\frac{1 + c_{w3}^6}{g^6 + c_{w3}^6} \right]^{1/6} \tag{5}$$

$$X = \frac{\bar{v}}{v} g = r + c_{w2} (r^6 - r), \quad r = \frac{\bar{v}}{\tilde{S} k^2 d^2} \tag{6}$$

$$\tilde{S} = S + \frac{\bar{v}}{k^2 d^2} f_{v2} S = \sqrt{2 \Omega_{ij} \Omega_{ij}} \tag{7}$$

2.5 Boundary Conditions

The analysis is carried out for Mach numbers 0.4, 06, 0.8 and 1.0. The corresponding total pressure for each Mach number is given as the inlet pressure whose values are1.13, 1.27, 1.5 and 1.89 bar. Ambient Pressure 1 bar is given as the nozzle exit condition and ambient temperature 300K is given as the operating temperature effects.

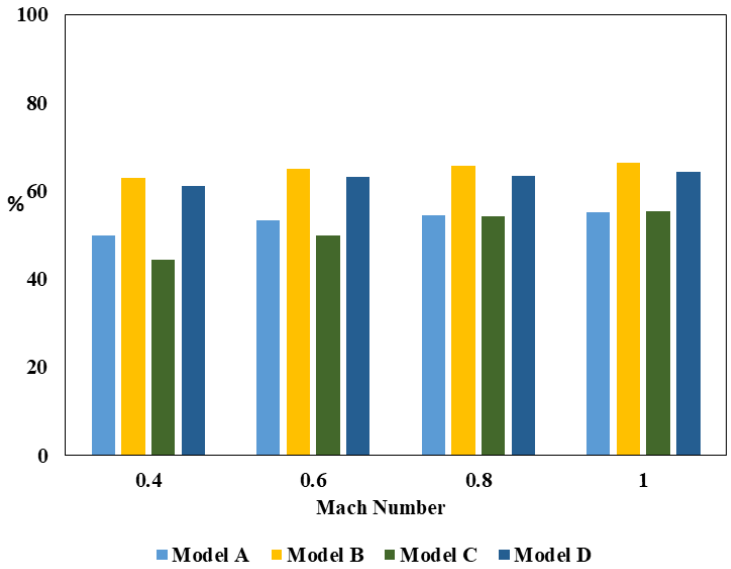

Fig. 7 Percentage of Reduction in potential core length

3. RESULTS AND DISCUSSION

3.1 Centreline Jet Characteristics

The centreline total pressure decay graph shows how the total pressure of the jet decays due to the jet mixing with the ambient fluid. Therefore, to understand the effect of the vanes on the jet mixing characteristics, the centreline total pressure decay is plotted for all the models considered. The total pressure values along the axial direction from the exit of the nozzle are non-dimensionalized with the inlet total pressure and the longitudinal distance is non-dimensionalized with the nozzle exit diameter. Shear layer is formed due to the mixing of the exhaust jet with the stationary ambient air at the nozzle exit due to the curvature, which causes the formation of vortices at the jet boundary. This process exchanges momentum between the exhaust jet and the ambient air. The uniform vortices formed at the nozzle exit which is proportional to the radius of curvature travel downstream by engulfing atmospheric air into the jet core which results in the decay of the potential core region. Since centreline total pressure decay is the measure of jet mixing, the faster the jet decay, the faster the jet mixes with the ambient air. The length of the potential core region at Mach numbers 0.4, 0.6, 0.8 and 1.0 for the base nozzle is 5.4D, 6D, 7D and 7.6D respectively and for Model A is 2.7D, 2.8D, 3.2D and 3.4D respectively and for Model B is 2D, 2.1D, 2.4D and 2.55D respectively and for Model C is 3D, 3D, 3.2D and 3.4D respectively and for Model D is 2.1D, 2.2D, 2.6D and 2.7D respectively. The potential core region is defined as the region where the total pressure of the jet is constant. Thus, a shorter core length indicates efficient mixing of the jet and the surrounding air.

Figure 7 shows the percentage of reduction in the potential core region for each nozzle model considered at various Mach numbers and Fig. 8 compares the centreline total pressure decay of the nozzle models at exit Mach numbers 0.4. It is observed that, the decay trend observed for Mach numbers 0.6, 0.8, and 1.0 are similar indicating consistent overall behavior of the decay process and thus the specific graphs for these Mach numbers are not presented in this analysis. This similarity refers to the general pattern of decay, rather than the specific length of the potential core region or the pressure values at particular locations. To present the results clearly, only three curves are plotted in a single graph.

It is observed that, when the vanes are introduced, the core length of the nozzle with vanes is reduced drastically as compared to the base nozzle for all the Mach numbers.

The vanes employed in this study have been found to induce a reduction in the potential core length, thereby generating tip vortices that promote the expansion of the jet boundary. Moreover, the implementation of vanes with varying widths along their length, as discussed by Rathakrishnan (2019) leads to the production of variable-sized vortices. The effect of vanes remains consistent from the near-field to the far-field region, as shown in Fig. 8a and 8b. At X/D = 5, the pressure ratio for the base nozzle is 0.98, while it is 0.6 for Model A, 0.5 for Model B, 0.53 for Model C, and 0.56 for Model D. Similarly, at X/D = 12.5, the base nozzle has a pressure ratio of 0.2, while Model A has 0.04, Model B has 0.05, Model C has 0.04, and Model D has 0.06. This consistent reduction in pressure ratios throughout the jet flow field highlights the efficiency of vanes as passive control elements for enhancing jet mixing and controlling flow characteristics. While control techniques such as notches and grooves (Vishnu & Rathakrishnan, 2003; Ishii et al., 2011), limiting tabs (Berrueta & Rathakrishnan, 2017), corrugated tabs (Rathakrishnan, 2013; Sathish & Senthilkumar, 2018; Akram & Rathakrishnan, 2019; Patil & Rathakrishnan, 2019), arc tabs (Thanigaiarasu et al., 2008; Chand et al., 2011), cross wire (Lovaraju & Rathakrishnan, 2006; Manigandan et al., 2018), perforated tabs (Ahmed et al., 2013) have shown efficacy in reducing the potential core length, they tend to exhibit a convergence in decay profiles between controlled and uncontrolled jets upon reaching the far-field. Consistent with these observations, our study corroborates the findings of Gandhinathan and Subramanian (2022).

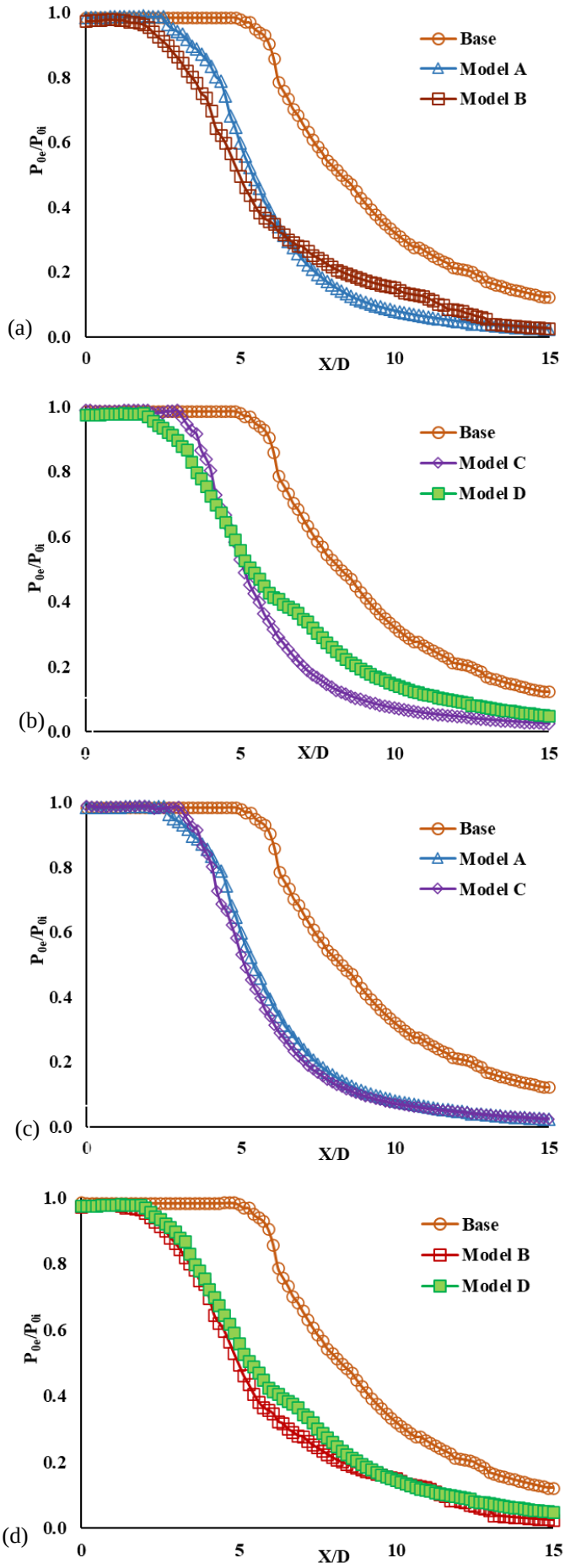

Fig. 8 Centerline Pressure Decay at M=0.4: a) Model A vs B, b) Model C vs D, c) Model A vs C, d) Model B vs D

It can be seen from the obtained results that model B has the most efficient design as the % reduction in potential core length for this particular nozzle design is about 66.4%. Comparing the centerline pressure decay results between the nozzle configurations with 12 vanes and 6 vanes (Fig. 8a and 8b) reveals interesting differences. Despite the presence of more vanes in the 12-vane configuration (Model A and C), the potential core length of the jet is still greater than that of the 6-vane configuration (Model B and D). One possible reason for the observed differences is the increased interaction and interference among the vortices in the 12-vane configuration. With a higher number of vanes and resulting vortices, there is a greater chance of complex vortex interactions, such as merging, cancellation, or suppression. These interactions can delay or hinder the core decay process, leading to a longer potential core length. Additionally, the closer spacing of vanes in the 12-vane configuration may result in a localized concentration of vortices, intensifying their interactions and further hindering core decay. In both the 12-vane and 6-vane configurations, the nozzle with vanes of 7.5mm length (model A and B) shows a higher reduction in the potential core length compared to the 5mm length vanes (model C and D). However, the difference in core length between the two lengths is relatively small, which could be attributed to the limited difference considered in this study. Future investigations with a more significant variation in vane lengths could provide a more comprehensive understanding of the length's effect on the potential core reduction.

3.2 Radial Pressure Decay

The total pressure is evaluated in the radial direction (along the Y and Z direction) at selected centreline distances such as X/D=0, X/D=5 and X/D=10. The radial pressure is plotted to get a clear picture of the jet spread and mixing in the radial direction.

Figure 9 and 10 compares the pressure decay of the nozzle models considered in the radial plane with that of the base nozzle. The pressure profile initially exhibits maximum pressure at the center (Y/D, Z/D = 0) and gradually decreases towards ambient conditions. As the flow reaches the vanes positioned at the nozzle exit, it encounters the stationary ambient fluid, leading to a diversion of the flow and the formation of vortices. This phenomenon can be attributed to the interaction between the flow and the vanes, which promotes enhanced mixing and facilitates a faster decay of the potential core (Gandhinathan & Subramanian, 2022).

Furthermore, the pressure decay curves of models A to E, which incorporate vanes, demonstrate a faster attainment of ambient pressure compared to the base nozzle at all X/D locations. This behavior can be attributed to the inclined and curved nature of the vanes, which induce a twisting effect on the jet, causing it to deviate away from the centerline (Billant et al., 1998). The extent of this twist depends on the geometric characteristics of the vanes, as highlighted by previous studies (Vignat et al., 2022).

The observed shift towards the positive Z-axis (Fig. 10) aligns with the rotational motion induced by the clockwise-oriented vanes, as reported in the study by Gandhinathan and Subramanian (2022). However, it is worth noting that a shift towards the negative Y-direction (Fig. 9) is also observed in this study, which was not explicitly discussed in their work. This unique shift can be attributed to the specific design and orientation of the vanes, where the vanes turn in a clockwise direction. Consequently, the jet itself rotates in a clockwise direction, leading to the observed displacement towards the negative Y-direction and positive Z-direction.

Interestingly, as the jet travels further downstream, the radial pressure decay results reveal a surprising trend. Despite the nozzle with 12 vanes initially having a greater potential core length compared to the nozzle with 6 vanes, at a specific axial location, the jet from the 12-vane configuration experiences a faster decay than the jet from the 6-vane configuration. This unexpected finding suggests that the interplay between vortices becomes more significant as the jet progresses in the downstream direction. The increased interaction and interference among the vortices generated by the additional vanes in the 12-vane configuration contribute to the accelerated decay rate. However, in the nearfield region, where the vortices are in closer proximity, the trend is reversed, with the 6-vane configuration showing a faster decay due to the specific arrangement and interaction of the vanes.

Furthermore, the effect of vane length on the core reduction process shows a discrepancy compared to the findings in the centerline pressure decay section. Contrary to expectations, the 5mm vane configuration exhibits a faster decay compared to the 7.5mm vane configuration. This contrasting trend may be attributed to the relatively small difference in vane length considered in this study. It is worth noting that the nearfield vortices interaction and the arrangement of vanes can have a pronounced effect on the decay process, resulting in different outcomes compared to the centerline behavior. However, as depicted in Figs 9 and 10, the pressure decay is consistently faster for the vaned nozzle compared to the base nozzle even as we move further away from the centerline along both Y and Z directions. This indicates that the vanes induce a more rapid pressure decay throughout the overall jet field, suggesting their effectiveness in enhancing mixing and controlling flow characteristics beyond the centerline region. To gain a more comprehensive understanding of the influence of vane length, future investigations should explore a wider range of vane length differences to assess their impact on the core reduction process more effectively. The decay trend for Mach numbers 0.6, 0.8, and 1.0 was found to have similarities, reflecting a consistent overall behavior in the decay process and hence the graphs corresponding to these Mach numbers are not included in this section. Again, this similarity refers to the general pattern of decay, rather than the specific total pressure values at particular locations.

3.3 Total Pressure Contour

The analysis of the total pressure contour in the YZ plane at x/d = 5, as depicted in Fig. 11, provides valuable insights into the radial characteristics of the jet flow at this

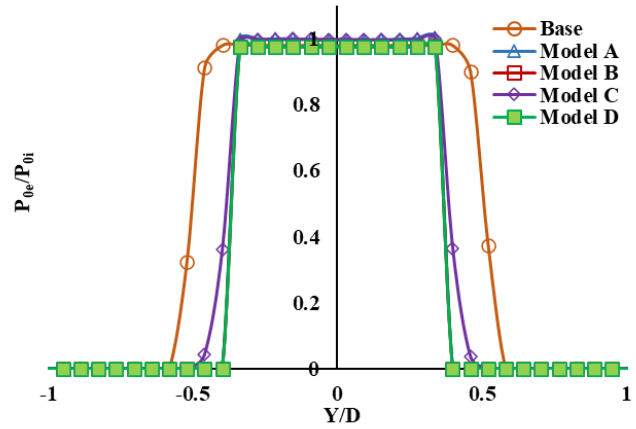

a)

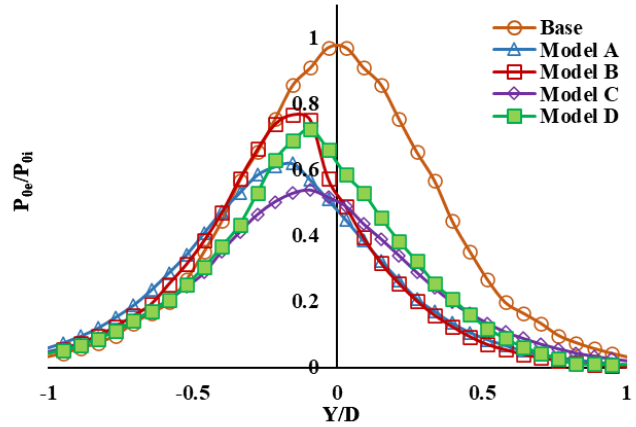

b)

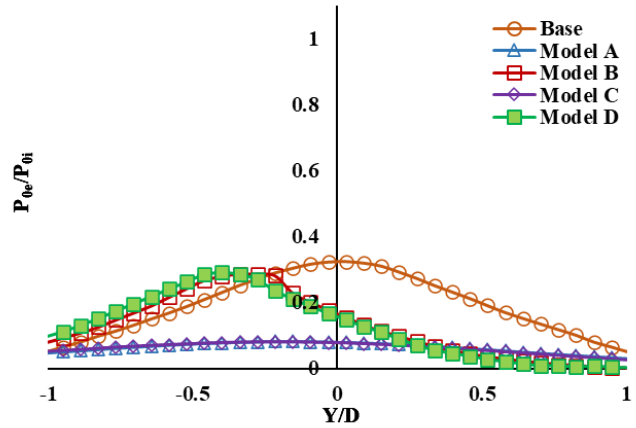

c)

Fig. 9 Radial Pressure Decay along Y direction at M=0.4: a) X/D = 0, b) X/D = 5, c) X/D = 10

specific location. The contour plot serves as a visual representation of the jet spread in the radial plane, showcasing the distribution of total pressure values. These contours further support the findings presented in the section 3.2, confirming the observed trends. It can be observed that the jet exhibits a shift towards the negative y-axis and positive z-axis, indicating the influence of the vane configuration on the flow trajectory. Moreover, the contour plot highlights the faster decay of the jet for models A to D compared to the base nozzle, in accordance with the conclusions discussed in section 3.2. Overall, the analysis of the total pressure contour adds a visual dimension to the understanding of the jet behavior and reinforces the findings obtained from the radial pressure decay analysis.

3.4 Thrust Loss

Since the vanes are placed inside the nozzle, they affect the exit pressure distribution and may cause thrust loss and it is necessary to determine the thrust loss caused by the vanes. The thrust force is directly proportional to the total pressure at the nozzle exit and hence by comparing the total pressure at the nozzle exit the model producing minimum thrust loss can be predicted.

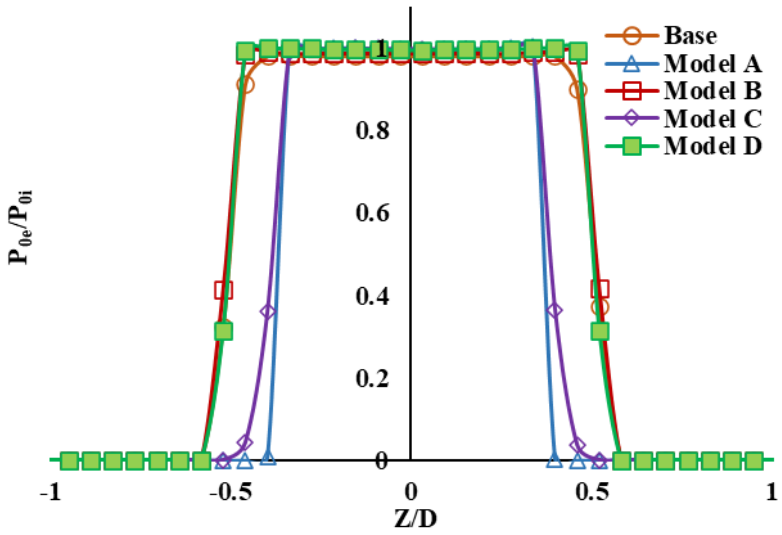

a)

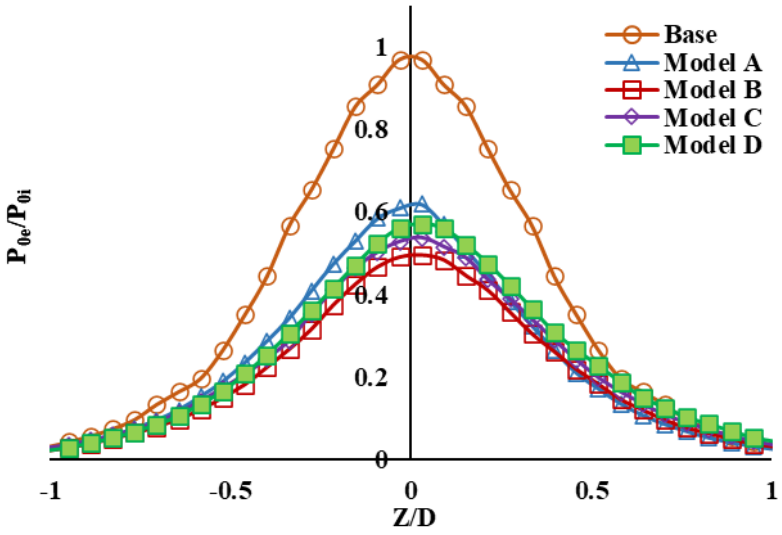

b)

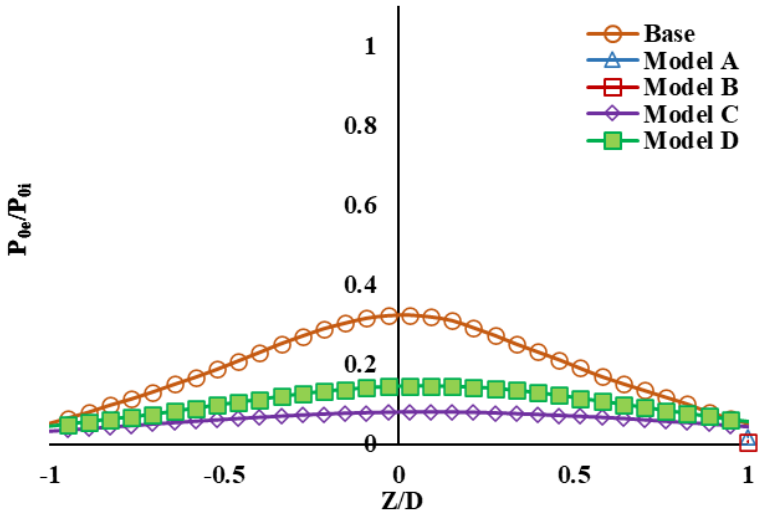

c)

Fig. 10 Radial Pressure Decay along Z direction at M=0.4: a) X/D = 0, b) X/D = 5, c) X/D = 10

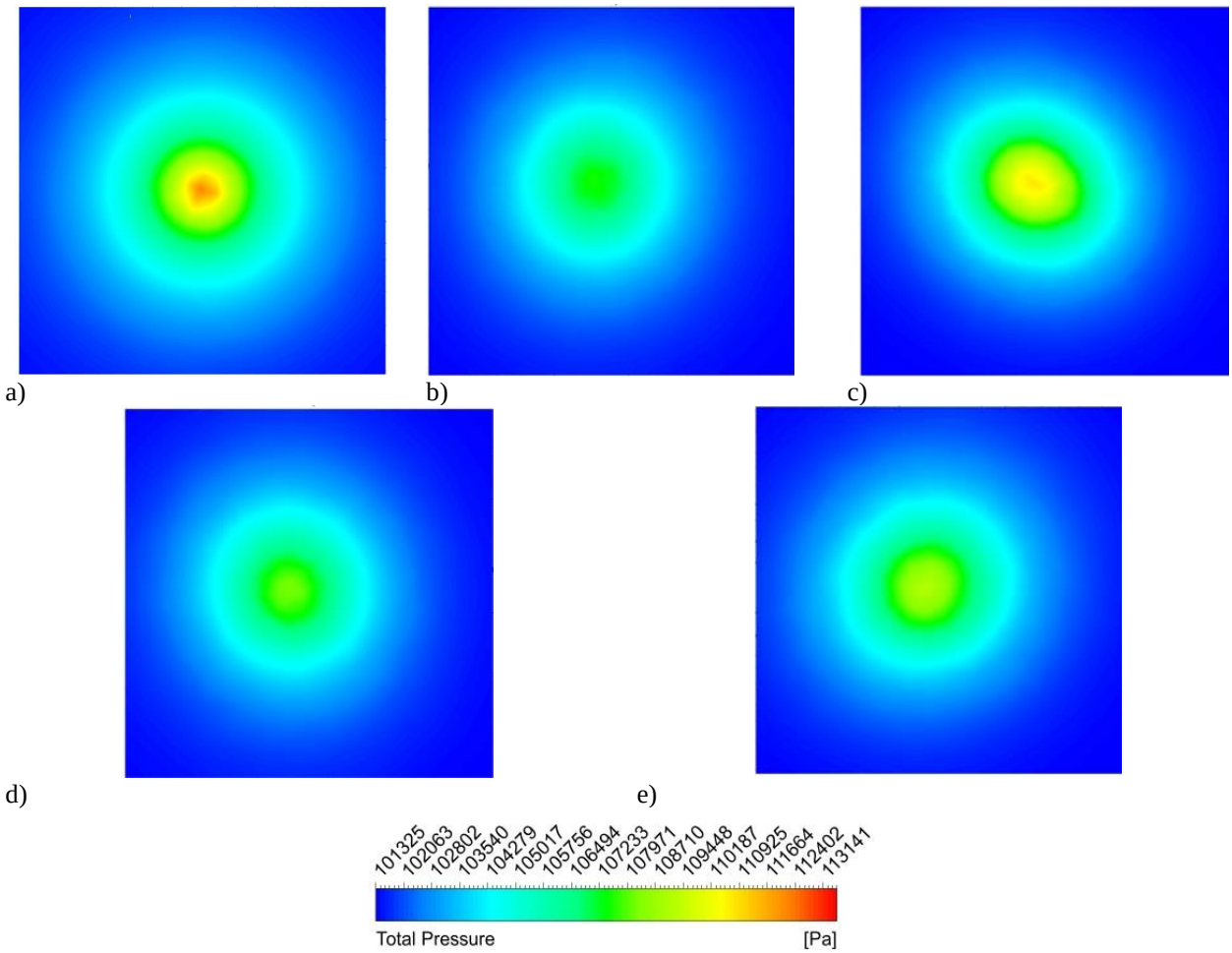

Fig. 11 Total Pressure Contour in YZ plane at M=0.4; X/D = 5: a) Base, b) Model A, c) Model B, d) Model C, e) Model D

Table 2 Total pressure loss at the Nozzle exit plane

Mach number	% Total pressure loss			
	Model A	Model B	Model C	Model D
0.4	1.09	0.63	0.78	0.47
0.6	2.21	1.34	1.64	1.02
0.8	2.53	1.82	2.1	1.58
1	2.98	2.26	2.64	1.95

The percentage of total pressure loss is calculated by comparing it with the base nozzle and the results are shown in Table 2. The amount of thrust loss caused due to the vanes is expected to be less as they are placed along the jet direction unlike other vortex generators like tabs which are placed normal to the flow causing sudden obstruction to the jet flow.

Model A, with 12 vanes of length 7.5 mm, experiences the highest total pressure loss. The larger number of vanes in Model A increases the obstruction to the flow, impeding the smooth movement of the jet and causing a greater pressure drop. In contrast, Model B, which has 6 vanes of the same length, exhibits a lower total pressure loss. The reduced number of vanes in Model B decreases the obstruction to the flow, allowing for better jet mixing and a lesser pressure drop. Moving on to Model C, despite having the same number of vanes as Model A, the shorter vane length of 5 mm reduces the obstruction to the flow. This leads to a further decrease in the total pressure loss compared to Models A and B. Finally, Model D, with 6 vanes of 5 mm length, experiences the lowest total pressure loss among the four models. The combination of fewer vanes and shorter length in Model D minimizes the obstruction to the flow, resulting in the smallest pressure drop at the nozzle exit.

3.5 Significance of Findings and Practical Implications

The findings of this study hold significant importance for enhancing mixing and minimizing thrust loss in jet applications and in the context of thrust vectoring applications. The observed reduction in potential core length achieved by using vanes demonstrates a promising passive control method for enhancing jet performance. One noteworthy finding is that the jet from the vaned nozzle moves away from the centerline towards the direction of the curvature of the vanes. This unique characteristic holds significant practical implications for the aerospace industry. By incorporating vanes into nozzle systems, engineers can achieve precise directional control of the jet, enhancing aircraft maneuverability and performance. Moreover, the quicker mixing and dispersion of the jet resulting from

vanes are crucial for optimizing combustion in gas turbines and exhaust systems, which can contribute to reducing noise and infrared signature emissions. Additionally, the minimal thrust loss observed with certain vane configurations can lead to improved fuel efficiency and reduced operational costs. Overall, this research offers valuable insights into the effectiveness of vane designs, providing practical guidelines for enhancing jet mixing while achieving thrust vectoring capabilities.

4. CONCLUSION

The analysis conducted on the jet decay using vanes has yielded several key findings.

Firstly, the centerline pressure decay plots clearly demonstrate that the inclusion of vanes results in a reduction of the potential core length. Model B exhibits the highest reduction, ranging from 62.9% to 66.4%.

Secondly, Model D exhibits the lowest total pressure loss at the nozzle exit ranging from 0.47% to 1.95%.

Furthermore, the radial pressure decay demonstrated that the jet from the nozzle with curved vanes tend to move away from the centreline towards the direction of curvature of the vanes.

The faster pressure decay of the jet from vaned nozzle is observed not only in the near field (X/D = 0 to 5) but also extends to the far field (X/D = 10 to 15) as observed in both centreline and radial pressure decay plots.

Model B stands out as the best design for efficient mixing, while Model D is recommended for minimizing thrust loss.

Nevertheless, the study acknowledges its limitations in terms of numerical simulations and emphasizes the need for carefully designed vane curvature for thrust vectoring applications while exploring a broader range of vane designs to gain more comprehensive understanding.

For future research, optimizing vane designs, exploring various parameters, and utilizing advanced techniques are proposed to achieve enhanced control and mixing capabilities, ultimately improving aircraft performance.

CONFLICT OF INTEREST

We hereby declare that we have no conflicts of interest to disclose regarding the publication of this manuscript. There are no financial or non-financial interests or relationships that could be perceived as potentially influencing the objectivity or integrity of the research presented in this study.

AUTHORS CONTRIBUTION

All four authors have made substantial and equal contributions to this work

REFERENCES

Akram, S., & Rathakrishnan, E. (2017). Control of supersonic elliptic jet with ventilated tabs. *International Journal of Turbo & Jet-Engines ISSN (Online)*, 2191–0332, ISSN. *Print* 0334-0082. https://doi.org/10.1515/tjj-2017-0033

Akram, S., & Rathakrishnan, E. (2019). Corrugated tabs for enhanced mixing of supersonic elliptic jet. *Journal of Aerospace Engineering*, 32(1), 04018140(1-14). https://doi.org/10.1061/(ASCE)AS.1943-5525.0000970

Aravindh, K. S. M., & Rathakrishnan, E. (2017). Control of elliptic supersonic jet of aspect ratio 3. *Journal of Aerospace Engineering*. 30(5), 1943-5525.0000762. https://doi.org/10.1061/(ASCE)

Ahmed, R. A., Thanigaiarasu, S., Santhosh, J., Elangovan, S., & Rathakrishnan, E. (2013). Study of slanted perforated jets. *International Journal of Turbo & Jet-Engines*, 30(4), 347–357. https://doi.org/10.1515/tjj-2013-0015

Berrueta, T., & Rathakrishnan, E. (2017). Control of subsonic and sonic jets with limiting tabs. *International Journal of Turbo and Jet-Engines*, 34(1), 103–113. https://doi.org/10.1515/tjj-2016-0037

Billant, P., Chomaz, J. M., & Huerre, P. (1998). Experimental study of vortex breakdown in swirling jets. *Journal of Fluid Mechanics*, 376, 183-219. https://doi.org/10.1017/S0022112098002870

Bradbury, L. J. S., & Khadem, A. H. (1975). The distortion of a jet by tabs. *Journal of Fluid Mechanics*, *70*(4), 801–813. https://doi.org/10.1017/S0022112075002352

Chand, D. S., Thanigaiarasu, S., Elangovan, S., & Rathakrishnan, E. (2011). Perforated arc-tabs for jet control. *International Journal of Turbo and Jet Engines*, 28(2), 133–138. https://doi.org/10.1515/tjj.2011.012

Chauvet, N., Deck, S., & Jacquin, L. (2007). Numerical study of mixing enhancement in a supersonic round jet. *AIAA Journal*, 45(7), 1675–1687. https://doi.org/10.2514/1.27497

Dhakshnamoorthy, M., Chand, D. S., Thanigaiarasu, S., & Elangovan, S. (2014, April 19–20). *Numerical simulation of subsonic jet control with perforated tabs*. International Conference on Recent Advances in Mechanical Engineering, Chennai, India.

Elangovan, S., & Rathakrishnan, E. (2004). Studies on high-speed jets from nozzles with internal grooves. *Aeronautical Journal*, 108(1079), 43–50. https://doi.org/10.1017/S000192400000498X

Ezhilmaran, G., Khandai, S. C., Sinha, Y. K., & Thanigaiarasu, S. (2019). Numerical simulation of supersonic jet control by tabs with slanted perforation. *International Journal of Turbo & Jet-Engines. ISSN (Online), 2191-0332, ISSN. Print 0334-0082* https://doi.org/10.1515/tjj-2019-0015

Gandhinathan, B., & Subramanian, T. (2022). Control of subsonic jets using vanes as vortex generators.

International Journal of Turbo and Jet-Engines. https://doi.org/10.1515/tjj-2022-0062

Ishii, T., Oinuma, H., Nagai, K., Tanaka, N., Oba, Y., & Oishi, T. (2011). *Experimental study on a notched nozzle for jet noise reduction.* Proceedings of the ASME Turbo Expo Vancouver, British Columbia, Canada. https://doi.org/10.1115/GT2011-46244

Jabez Richards, S. B., Thanigaiarasu, S., & Kaushik, M. (2023). Experimental study on the effect of tabs with asymmetric projections on the mixing characteristics of subsonic jets. *Journal of Applied Fluid Mechanics*, 16(6), 1208–1217. https://doi.org/10.47176/jafm.16.06.1584

Lovaraju, P., & Rathakrishnan, E. (2006). Subsonic and transonic jet control with cross-wire. *AIAA Journal*, 44(11), 2700–2705. https://doi.org/10.2514/1.17637

Mali, A. K., Jana, T., Kaushik, M., & Mishra, D. P. (2023). Influences of semi-circular, square, and triangular grooves on mixing behavior of an axisymmetric supersonic jet. *Physics of Fluids*, 35(4). https://doi.org/10.1063/5.0146672

Manigandan, S., Vijayaraja, K., Durga Revanth, G., & Anudeep, A. V. S. C. (2018). *Mixing and entrainment characteristics of jet control with crosswire*. *Advances in Machine Learning and Data Science* (pp. 121–128). https://doi.org/10.1007/978-981-10-8569-7_13

Maruthupandiyan, K., & Rathakrishnan, E. (2018). Shifted triangular tabs for supersonic jet control. *Journal of Aerospace Engineering*, 31(5), 04018067(1-8). https://doi.org/10.1061/(ASCE)AS.1943-5525.0000893

Naren, S. R., Thanigaiarasu, S., & Rathakrishnan, E. (2016). Numerical characterization of lip thickness on subsonic and correctly expanded sonic co-flowing jets. *Transactions of the Japan Society for Aeronautical and Space Sciences*, 59(3), 134–141. https://doi.org/10.2322/tjsass.59.134

Pannu, S. S., & Johannesen, N. H. (1976). The structure of jets from notched nozzles. *Journal of Fluid Mechanics*, 74(3), 515–528. https://doi.org/10.1017/S0022112076001924

Patil, R., & Rathakrishnan, E. (2019). Sonic elliptic jet control with corrugated limiting tab. *Journal of Aerospace Engineering*, 32(2), 04018151(1-18). https://doi.org/10.1061/(ASCE)AS.1943-5525.0000976

Powell, A. (1954). The reduction of choked jet noise. *Proceedings of the Physical Society. Section B*, 67(4), 313–327. https://doi.org/10.1088/0370-1301/67/4/306

Rathakrishnan, E. (2013). Corrugated tabs for subsonic and sonic jet control. *Journal of Aeronautics and Aerospace Engineering*, 02(5). https://doi.org/10.4172/2168-9792.1000120

Rathakrishnan, E. (2019). *Applied gas dynamics*. John Wiley & Sons.

Reddy, D. R., & Zaman, K. B. M. Q. (2006). Computational study of effect of tabs on a jet in a cross flow. *Computers and Fluids*, 35(7), 712–723. https://doi.org/10.1016/j.compfluid.2006.01.011

Sathish, K. K., & Senthilkumar, C. (2018). Jet flow control using semi-circular corrugated tab. *International Journal of Turbo & Jet-Engines* https://doi.org/10.1515/tjj-2018-0014

Spalart, P. R., & Allmaras, S. R. (1992). *A one-equation turbulence model for aerodynamic flows* In 30th aerospace sciences meeting and exhibit (pp. 92–0439). https://doi.org/10.2514/6.1992-439

Suseela Moorthi, A. K., Perumal, A. K., & Rathakrishnan, E. (2023). Jet mixing manipulation with asymmetric orientation of tabs. *Proceedings of the Institution of Mechanical Engineers, Part G*, 237(7), 1571–1581. https://doi.org/10.1177/09544100221132653

Thangaraj, T., Kaushik, M., Deb, D., Unguresan, M., & Muresan, V. (2022). Survey on vortex shedding tabs as supersonic jet control. *Frontiers in Physics*, 9, 789742. https://doi.org/10.3389/fphy.2021.789742

Thanigaiarasu, S., Jayaprakash, S., Elangovan, S., & Rathakrishnan, E. (2008). Influence of tab geometry and its orientation on under-expanded sonic jets. *Proceedings of the IMech e Part G. Proceedings of the Institution of Mechanical Engineers, Part G*, 222(3), 331–339. https://doi.org/10.1243/09544100JAERO299

Vignat, G., Durox, D., & Candel, S. (2022). The suitability of different swirl number definitions for describing swirl flows: Accurate, common and (over-) simplified formulations. *Progress in Energy and Combustion Science*, 89, 100969.

Vishnu, J., & Rathakrishnan, E. (2003). *Jets from grooved nozzles*. Proceedings of the 39thAIAA/ASME/SAE/ASEE Joint Propulsion Conference and Exhibit Huntsville, Alabama. AIAA, 4402. https://doi.org/10.2514/6.2003-4402

Wan, C., & Yu, S. C. M. (2013). Numerical investigation of the air tabs technique in jet flow. *Journal of Propulsion and Power*, 29(1), 42–49. https://doi.org/10.2514/1.B34534

Wilcox, D. C. (1993). *Turbulence modeling for CFD*. DCW Industries, Inc.